X-721-65-335

NASA TM X-55282

A THEORETICAL INVESTIGATION OF THE ROLLING MOTION OF THE NIKE CAJUN AND NIKE APACHE ROCKET VEHICLES

BY

ROGER J. HAWKS

AUGUST 1965

NASA — GODDARD SPACE FLIGHT CENTER

GREENBELT, MARYLAND

A THEORETICAL INVESTIGATION OF THE ROLLING MOTION OF THE NIKE CAJUN AND NIKE APACHE ROCKET VEHICLES

By

Roger J. Hawks

National Aeronautics and Space Administration
Goddard Space Flight Center
Greenbelt, Maryland

ACKNOWLEDGEMENT

The following paper was originally published as a thesis submitted to the Faculty of the College of Engineering, University of Cincinnati, in partial fulfillment of the requirements for the degree of Bachelor of Science in Aerospace Engineering, 1965.

TABLE OF CONTENTS

SYMBOLS

A	Total wedge height $A = \Delta + 0.062$ in
AR	Aspect ratio
C_1, C_2, C_3, D	Coefficients for Busemann equation
C_{L_α}	Fin lift-curve slope
C_l	Rolling moment coefficient $C_l = \frac{L}{qdS_B}$
C_l'	Roll forcing moment coefficient
C_{l_p}	Roll damping moment
C_{l_δ}	Roll forcing derivative
C_P	Pressure coefficient
F	Aerodynamic force
I_{xx}	Moment of inertia about longitudinal axis
L	Rolling Moment
M	Mach number
Re_x	Local Reynolds number $Re_x = \frac{\rho Vx}{\mu}$
S	Area of fin
S_B	Body cross-sectional area $S_B = \frac{\pi d^2}{4}$
S_W	Area on fin used to determine velocity potential
U	Local velocity of potential flow
V	Free stream velocity
a	Shroud Diameter

b	Fin span
c	Fin chord
d	Body diameter
h	Wedge chord
m	Wedge shape parameter
p	Roll rate
q	Dynamic pressure $q = 1/2 \rho V^2$
s	Fin semi-span $s = 1/2b$
u	Local velocity in x direction
u_o	Perturbation velocity in x direction
x	Coordinate parallel to longitudinal axis
y	Coordinate normal to longitudinal axis along fin
z	Coordinate normal to fin
Γ	Supersonic source strength
Δ	Wedge height $\Delta = h \tan \delta$
ϕ	Roll angle
α	Angle of attack
β	Compressibility factor $\beta = \sqrt{\lvert M^2 - 1 \rvert}$
δ	Wedge angle
δ'	Boundary layer thickness
λ	Fin taper ratio $\lambda = \frac{c_t}{c_r}$

ρ	Local air density
σ	Fin mid-chord sweepback angle
ξ	General chord-wise coordinate of point on fin
η	General span-wise coordinate of point on fin
μ	Local air viscosity
φ	Velocity potential

SUBSCRIPTS

SS	Steady-stage
p	Roll
r	Root
t	Tip
δ	Wedge

A THEORETICAL INVESTIGATION OF THE ROLLING MOTION OF THE NIKE CAJUN AND NIKE APACHE ROCKET VEHICLES

SUMMARY

32572

An attempt has been made to theoretically predict the roll rate of the second stage of the Nike Cajun and Nike Apache sounding rocket vehicles. The one-degree-of-freedom roll equation was derived. General expressions were obtained for the roll damping coefficient derivative of a sounding rocket in both subsonic and supersonic flight. Analytic expressions for the roll forcing moment coefficient due to fin trailing-edge wedges are presented for the subsonic and supersonic flight regimes.

These equations have been applied to the Cajun and Apache vehicles and the results compared to wind tunnel and free-flight test results. The roll damping coefficients are in excellent agreement with wind tunnel results, but the roll forcing coefficients do not agree. Neither the theoretical nor the wind tunnel forcing coefficients gave a roll history as obtained in free-flight tests. The theoretically predicted roll history does, however, show several previously unexplained characteristics of the free-flight roll history.

Author

INTRODUCTION

The Nike Cajun and Nike Apache are two-stage, unguided sounding rockets used by NASA for upper atmosphere and meteorological research. The first stage of both vehicles is a solid-propellant Nike M5-E1 booster. This booster burns for 3.5 seconds. The second stage is fired 16 seconds after first stage burnout and burns four (4) seconds for the Cajun or 6.5 seconds for the Apache. The Nike Cajun can lift an 80 pound payload approximately 100 miles and the Nike Apache will achieve an apogee of 150 miles with the same payload.

Except for the propellant and the nozzle, the Cajun and the Apache vehicles are identical. As the Cajun and Apache vehicles are geometrically identical, aerodynamically they can be considered to be the same vehicle, which is usually called the Capache vehicle. This practice will be followed hereafter when referring to the general vehicle.

The Capache vehicle has a diameter of 6.5 inches and a fin span of 25.5 inches. It is equipped with four (4) cruciform fins whose planform is best described as swept-back and tapered with streamwise tips. Under normal second stage Capache flight conditions the leading and trailing edges are supersonic. The fins are mounted on a shroud having a diameter of 7.5 inches. Figure 1 is a sketch of the Capache vehicle.

As the Nike Cajun is unguided it must be spin-stabilized to attain good payload attitude in space. Roll is achieved in the Capache vehicle by mounting spin tabs or wedges on the trailing edges of all four fins. The wedges extend full span and roll rate control is obtained by changing the values of wedge angle and wedge area. It is most convenient to use wedges of a given constant chord, thereby reducing the control problem to only one parameter, wedge height. Wedge dimensions and placement are shown in Figure 2.

When the magnitudes of the roll rate and the pitch frequency are similar, a pitch-roll coupling occurs. This coupling usually results in pitch-roll resonance or "roll lock-in". Roll lock-in produces unstable flight and, if the dynamic pressure is sufficiently high, is often catastrophic. Calculations of typical pitch frequencies show that the theoretical rigid body pitch frequency of the Capache vehicle is above 5 cycles per second at second stage separation, decays to 2 cycles per second at second stage ignition, peaks at 2.5 cycles per second just before Capache burnout, and then decays asymptotically to zero (Figure 3).

Two methods are available for preventing pitch-roll resonance. The first is to hold the roll rate as close to zero as possible. This method, however, often results in poor vehicle attitude in space. In order to obtain good attitude in space, the vehicle must be rolled. To prevent roll lock-in the roll rate should pass through the lock-in point (where the roll rate and pitch frequency are equal) with as high a roll acceleration as possible. The roll rate at Capache burnout should also be at least 5 rps to prevent lock-in at that time.

DERIVATION OF THE ROLL EQUATION

The rolling motion of a rocket vehicle is described by the basic dynamic equation

$$I_{xx} \ddot{\phi} = L \tag{1}$$

The rolling moment L is the sum of three terms, the forcing moment, the damping moment, and the induced moment. The forcing moment is a function of control deflection (or wedge angle) δ, the damping moment is a function of roll rate $\dot{\phi}$, and the induced moment is a function of angle of attack α and roll angle ϕ. For the purposes of this analysis, the angle of attack is assumed to be zero so that there are no induced rolling moments. (For roll lock-in to occur there must be induced

rolling moments present. However, this analysis is interested in determining the roll rate and is not designed to analyze roll lock-in other than to avoid its occurrence.)

Under this linear theory, two rolling moment coefficient derivatives are defined. These derivatives, the forcing derivative and the damping derivative are defined as follows:

(a) Forcing moment coefficient:

$$C_{l_\delta} = \frac{\partial}{\partial \delta}\left(\frac{L_\delta}{q d S_B}\right) \tag{2}$$

(b) Damping moment coefficient:

$$C_{l_p} = \frac{\partial}{\partial\left(\frac{\dot{\phi} d}{2V}\right)}\left(\frac{L_p}{q d S_B}\right)\Bigg|_{\frac{\dot{\phi} d}{2V} \to 0} \tag{3}$$

Therefore,

$$L = C_{l_\delta}\, \delta\, q d S_B + C_{l_p} \frac{\dot{\phi} d}{2V}\, q d S_B \tag{4}$$

Substituting into equation (1), simplifying and changing variables gives

$$I_{xx}\, \dot{p} = \left(C_{l_\delta}\, \delta + C_{l_p} \frac{p d}{2V}\right) q d S_B \tag{5}$$

Wind tunnel test results give the term $C_{l_\delta}\delta$ as a function of Mach number. The term is defined to be identical with C_l' for the purposes of this analysis. That is,

$$C_l' \equiv C_{l_\delta}\, \delta \tag{6}$$

For a steady-state rolling motion

$$\dot{p} = 0 \tag{7}$$

if I_{xx} is finite. Therefore,

$$p_{ss} = -\frac{C_\ell'}{C_{\ell_p}} \frac{2V}{d} \tag{8}$$

Equations (5) and (8) have been programmed for solution on a digital computer.

CALCULATION OF ROLL DAMPING COEFFICIENT

The next step of the analysis involves determination of the rolling moment coefficients. As the Capache vehicle normally operates with the leading edges of the fins supersonic, values of the coefficients for Mach numbers less than 1.4 are needed only to show trends and do not require a high degree of accuracy. Therefore, simple strip theory will be used for the subsonic regime.

Considering a chordwise strip (Figure 4),

$$L_p = -\int_0^s y C_{L_\alpha} \frac{py}{V} qc \, dy \tag{9}$$

Substituting for the general chord in terms of taper ratio and non-dimensionalizing gives

$$C_\ell = -\frac{C_{L_\alpha} c_r}{d S_B} \frac{p}{V} \int_0^s y^2 \left(1 - \frac{1-\lambda}{s} y\right) dy \tag{10}$$

which, upon integrating results in

$$C_{\ell} = -\frac{C_{L\alpha}\, c_r}{d S_B}\,\frac{p s^3}{V}\left(\frac{1+3\lambda}{12}\right) \tag{11}$$

Thus,

$$C_{\ell_p} = -\frac{C_{L\alpha}\, c_r\, s^3}{d^2\, S_B}\left(\frac{1+3\lambda}{6}\right) \tag{12}$$

For a flat plate in incompressible flow, the lift-curve slope is 2π. Correcting for compressibility, sweepback, and aspect ratio (Ref. 1) the lift-curve slope becomes

$$C_{L\alpha} = \frac{2\pi A \cos\sigma}{2\cos\sigma + \sqrt{(\beta A)^2 + 4\cos^2\sigma}} \tag{13}$$

Combining equations (12) and (13) for a four finned vehicle gives

$$C_{\ell_p} = -\frac{2 c_r s^3 (1+3\lambda)}{3 d^2 S_B}\,\frac{\pi A \cos\sigma}{\cos\sigma + \frac{1}{2}\sqrt{(\beta A)^2 + 4\cos^2\sigma}} \tag{14}$$

The damping moment on a supersonic fin is given by

$$L_p = -\iint_S C_p\, y\, dy\, dx \tag{15}$$

where C_p is an unknown function,

$$C_p = f(x, y, p, M, V, \alpha) \tag{16}$$

Thus,

$$C_{l_p} = -\frac{1}{q dS_B} \frac{\partial}{\partial\left(\frac{pd}{2V}\right)} \iint_S C_p \, y \, dy \, dx \tag{17}$$

From the linearized Bernoulli equation,

$$C_p = \frac{2\rho V u_o}{q} \tag{18}$$

or simply,

$$C_p = \frac{4 u_o}{V} \tag{19}$$

The perturbation velocity is most easily found by replacing the fin with a distributed sheet of supersonic sources. The perturbation velocity is then given by the X-derivative of the velocity potential of these sources. That is,

$$u_o = \frac{\partial \varphi}{\partial x} \tag{20}$$

Hence,

$$C_p = \frac{4}{V} \frac{\partial \varphi}{\partial x} \tag{21}$$

The velocity potential of the distributed sources is (Ref. 2),

$$\varphi = \frac{V}{\pi} \iint_{S_w} \frac{\Gamma \, d\xi \, d\eta}{\sqrt{(x-\xi)^2 - \beta^2 (y-\eta)^2}} \tag{22}$$

where Γ is the source strength, and S_w is some region on the fin defined by intersections between the Mach forecone of the point (ξ, η) and the edges of the fin (Figure 5). The pressure coefficient is therefore

$$C_p = \frac{4}{\pi} \frac{\partial}{\partial x} \iint_{S_w} \frac{\Gamma \, d\xi \, d\eta}{\sqrt{(x-\xi)^2 - \beta^2 (y-\eta)^2}} \tag{23}$$

For a rolling fin at zero angle of attack the source strength is

$$\Gamma = \frac{p \eta}{V} \tag{24}$$

Therefore,

$$C_p = \frac{4p}{\pi V} \frac{\partial}{\partial x} \iint_{S_w} \frac{\eta \, d\eta \, d\xi}{\sqrt{(x-\xi)^2 - \beta^2 (y-\eta)^2}} \tag{25}$$

Combining equation (25) with equation (17) gives

$$C_{x_r} = -\frac{1}{q S_B} \frac{\partial}{\partial \left(\frac{pd}{2V}\right)} \left\{ \frac{4p}{\pi V} \iint_S y \left[\frac{\partial}{\partial x} \iint_{S_w} \frac{\eta \, d\eta \, d\xi}{\sqrt{(x-\xi)^2 - \beta^2 (y-\eta)^2}} \right] dy \, dx \right\} \tag{26}$$

The rather cumbersome integrations of equation (26) have been carried out by Malvestuto et al (Ref. 3) for the case of subsonic leading edges and by Harmon and Jeffreys (Ref. 4) for the supersonic leading edges. In both cases the results have been presented as design charts. These charts have been used here to determine the damping moment coefficients as needed.

The above method, equation (26), neglects the effects of fin-body interference. This is in keeping with the standard practice of neglecting body effects when the ratio of body radius to fin semi-span is less than 0.30. If it is desirable to include body effects, equation (24) can be modified to

$$\Gamma = \frac{p}{V} \left[a - \left(\frac{2a\beta}{C_r + a\beta} - 1 \right) (\eta - a) \right] \tag{27}$$

for $\eta < a$ (Ref. 5).

The damping moment coefficient for the Capache as computed from equations (13) and (26) was compared with data taken in wind-tunnel tests (Ref. 6). Excellent agreement resulted (Figure 6).

CALCULATION OF ROLL FORCING COEFFICIENT

The flow field over the wedge producing the forcing moment is quite complex, and straightforward mathematical solutions are not available as above. The various Mach lines emanating from the leading edge root and tip intersect in such a manner that at low Mach numbers none of the wedge experiences two-dimensional flow, and at higher Mach numbers only a small portion of the wedge experiences two-dimensional flow (Figure 7). According to Evvard's linear aerofoil theory, however, these Mach lines do not affect the two-dimensional nature of the flow at zero angle of attack. The only portion of the wedge that would deviate from two-dimensional flow would be in the regions behind the Mach lines emanating from the junctions of the leading edge of the wedge with the body and the tip. These regions are negligible when compared to the total area of the wedge.

A further complication of the flow over the wedge is due to the presence of the boundary layer. By assuming that a local Reynolds number of 5×10^5 is sufficient to assure a turbulent boundary layer, and making the added and rather gross assumption that the Inconel cap on the leading edge of the fin acts as a trip, the general statement can be made that the boundary layer in the vicinity of the wedge is of a fully developed turbulent nature.

For the purpose of boundary layer calculations, a 1/5 power velocity distribution was assumed for the turbulent boundary layer:

$$\frac{u}{V} = \left(\frac{z}{\delta'}\right)^{\frac{1}{5}} \tag{28}$$

For this velocity distribution the boundary layer thickness is (Ref. 7)

$$\frac{\delta'}{X} = 0.1285 \left(Re_x\right)^{-\frac{1}{7}} \tag{29}$$

A boundary layer thickness history was prepared for a typical Apache trajectory using the boundary layer thickness at the tip of the trailing edge. This point is the point of minimum boundary layer thickness on the wedge. From this history (Figure 8) it was determined that, even at minimum boundary layer thickness, the boundary layer thickness is greater than wedge height.

Another point to be considered is boundary layer separation in the compression corner formed by the intersection of the wedge with the fin. This separation and the subsequent reattachment produce an additional shock wave. An oblique shock is formed at the separation point and another oblique shock is formed at the reattachment point. This deviates from the ideal flow case of one oblique shock extending from the corner. Kuehn (Ref. 8) has measured the pressure distributions produced by separation of turbulent boundary layers in such corners. By numerically integrating the measured pressure distribution to obtain the resultant force per unit width, it has been determined that viscous effects in general reduced the resultant force acting by 5% from the ideal value, regardless of whether separation occurs in the corner. Thus, boundary layer effects will be generally ignored in computing forcing moments.

The aerodynamic force on the wedge is given by

$$dF_\delta = C_p \, q \, dy \, dx \tag{30}$$

and the rolling moment is

$$L_\delta = \int_0^h \int_a^s C_p \, q \, y \, dy \, dx \tag{31}$$

For incompressible flow,

$$C_p = 1 - \left(\frac{U}{V}\right)^2 \tag{32}$$

by Bernoulli's equation. From potential flow theory (Ref. 9),

$$U = V x^{m} \tag{33}$$

where

$$m = \frac{\delta}{\pi - \delta} \tag{34}$$

Thus,

$$C_p = 1 - x^{\frac{2\delta}{\pi-\delta}} \tag{35}$$

for incompressible flow. Applying the Prandtl-Glauert rule for compressible subsonic flow gives

$$C_p = \frac{1}{\beta}\left(1 - x^{\frac{2\delta}{\pi-\delta}}\right) \tag{36}$$

Substituting into equation (31) gives

$$L_\delta = \int_0^h \int_a^s \frac{q}{\beta}\left(1 - x^{\frac{2\delta}{\pi-\delta}}\right) y \, dy \, dx \tag{37}$$

and hence

$$C_l' = \frac{s^2 - a^2}{2d S_B \beta}\left[h - \frac{\pi - \delta}{\pi + \delta} h^{\frac{\pi+\delta}{\pi-\delta}}\right] \tag{38}$$

as the forcing moment coefficient for subsonic flow.

The pressure coefficient for supersonic flow is in general given by Busemann's oblique shock equation for two-dimensional flow:

$$C_p = C_1\delta + C_2\delta^2 + C_3\delta^3 + \cdots \tag{39}$$

Two approximations to the Busemann equation are in use. The linear form is the well-known Ackeret equation

$$C_p = \frac{2}{\beta}\delta \tag{40}$$

and a third-order form due to Bonney (Ref. 10) is

$$C_p = C_1\delta + C_2\delta^2 + (C_3 - D)\delta^3 \tag{41}$$

Both approximations were used with equation (31) to generate forcing moment coefficients. It was found that the linear form gave a better agreement with the wind tunnel data. Substituting equation (40) into equation (31) and integrating gives

$$C_l' = \frac{\delta h}{\beta d S_B}\left(s^2 - a^2\right) \tag{42}$$

or

$$C_{l_\delta} = \frac{h\left(s^2 - a^2\right)}{\beta d S_B} \tag{43}$$

The forcing moment generated by equations (38) and (43) is plotted in Figure 9, along with wind tunnel data for a representative value of δ. Agreement between theoretical and wind tunnel data is not good.

RESULTS

Both theoretical and wind tunnel forcing moment coefficients were used to predict the roll histories of several Capache flights. Neither set of coefficients produced a roll history which agreed with the measured flight roll rate (Figure 10). At some portions of the flight the predicted values were as much as 60% in error compared to the flight measured values. All attempts to correlate the differences between predicted roll rates and measured flight values with flight parameters have failed.

Several effects are probably responsible for these discrepancies. There is evidence that aeroelastic and jet plumage effects have a strong effect on the flight roll rate. Also the effect of the boundary layer on the roll rate cannot be discounted. Boundary layer was ignored in the theoretical calculations carried out here. The Reynolds number in the wind tunnel tests was much lower than the flight Reynolds numbers. Thus, in the wind tunnel tests, the boundary layer build-up was not representative of flight cases.

CONCLUSIONS

1. Although the equations derived here do not give a highly accurate description of the roll history of the Nike Capache vehicle in flight, they are a definite improvement on the equations used by Cooper and Mamone (Ref. 11) and by Jenkins (Ref. 12).

2. The equations, as derived here, while not accurate enough for a roll lock-in study, do give sufficiently accurate roll rate predictions for general use in planning the payload requirements for the experiment and the telemetry.

REFERENCES

1. Shapiro, Ascher H., The Dynamics and Thermodynamics of Compressible Fluid Flow, Volume 1, Ronald Press, New York, 1953.

2. Evvard, John C., NACA TN 1382, "Distribution of Wave Drag and Lift in the Vicinity of Wing Tips at Supersonic Speeds", Washington, July 1947.

3. Malvestuto, Frank S., Jr., Kenneth Margolis, and Herbert S. Ribner, NACA Rept. 970, "Theoretical Lift and Damping in Roll at Supersonic Speeds of Thin Sweptback Tapered Wings with Streamwise Tips, Subsonic Leading Edges, and Supersonic Trailing Edges", Washington, 1950.

4. Harmon, Sidney M. and Isabella Jeffreys, NACA TN 2114, "Theoretical Lift and Damping in Roll of Thin Wings with Arbitrary Sweep and Taper at Supersonic Speeds, Supersonic Leading and Trailing Edges", Washington, May 1950.

5. Tucker, Warren A. and Robert O. Piland, NACA TN 2151, "Estimation of the Damping in Roll of Supersonic-leading-edge Wing-body Combinations", Washington, July 1950.

6. Falanga, Ralph A., NASA TN D-2576, "Supersonic Investigation of a Spinning and Nonspinning Model of a Cajun (or Apache) Rocket Vehicle with Roll-control Tabs", Washington, January 1965.

7. Tabakoff, Widen, Unpublished Lectures on "Viscous Flow", University of Cincinnati, 1963.

8. Kuehn, Donald M., NASA MEMO 1-21-59A, "Experimental Investigation of the Pressure Rise Required for the Incipient Separation of Turbulent Boundary Layers in Two-Dimensional Supersonic Flow", Washington, February 1959.

9. Schlichting, Hermann, Boundary Layer Theory, 4th Ed., McGraw-Hill, New York, 1960.

10. Bonney, E. Arthur, Engineering Supersonic Aerodynamics, McGraw-Hill, New York, 1950.

11. Cooper, Earl and Russell Mamone, Atlantic Research Corporation, Space Vehicles Group Report 7903-2-01, "Feasibility Study Nike Apache Rocket System with Fiberglass Payload", Pasadena, California, 30 April 1961.

12. Jenkins, Reed B., "Cajun-Apache Roll Rate", Unpublished Report, Goddard Space Flight Center.

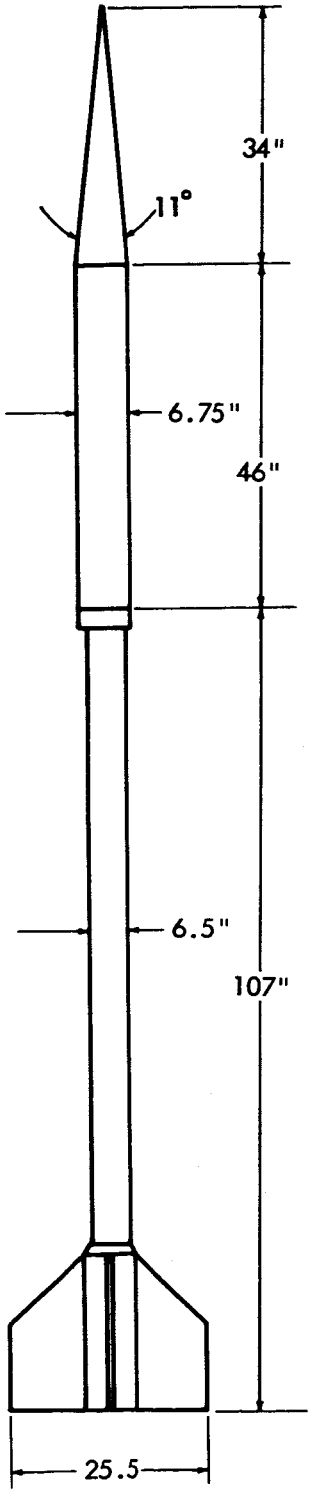

Figure 1 - Capacne Vehicle

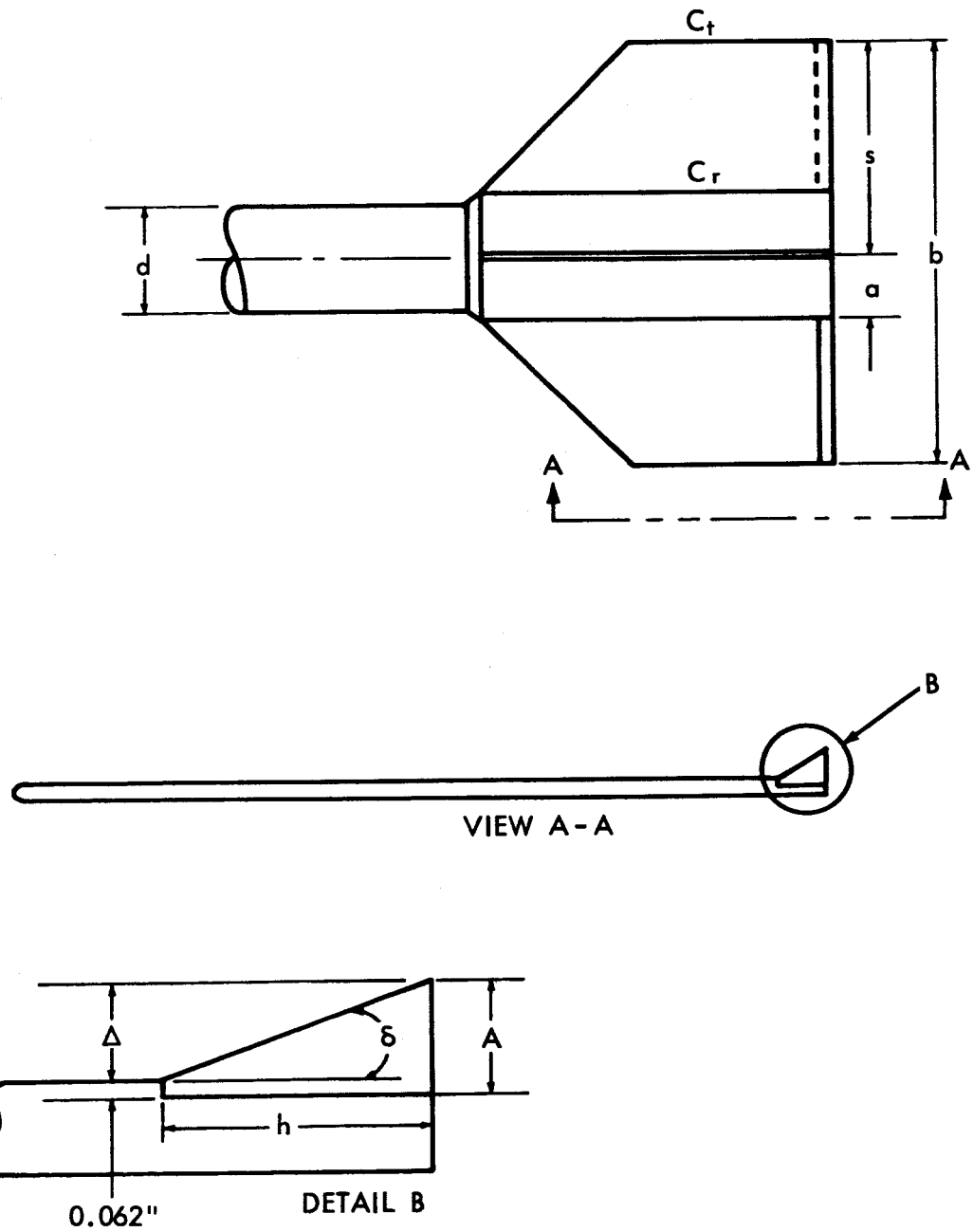

Figure 2- Spin Tab

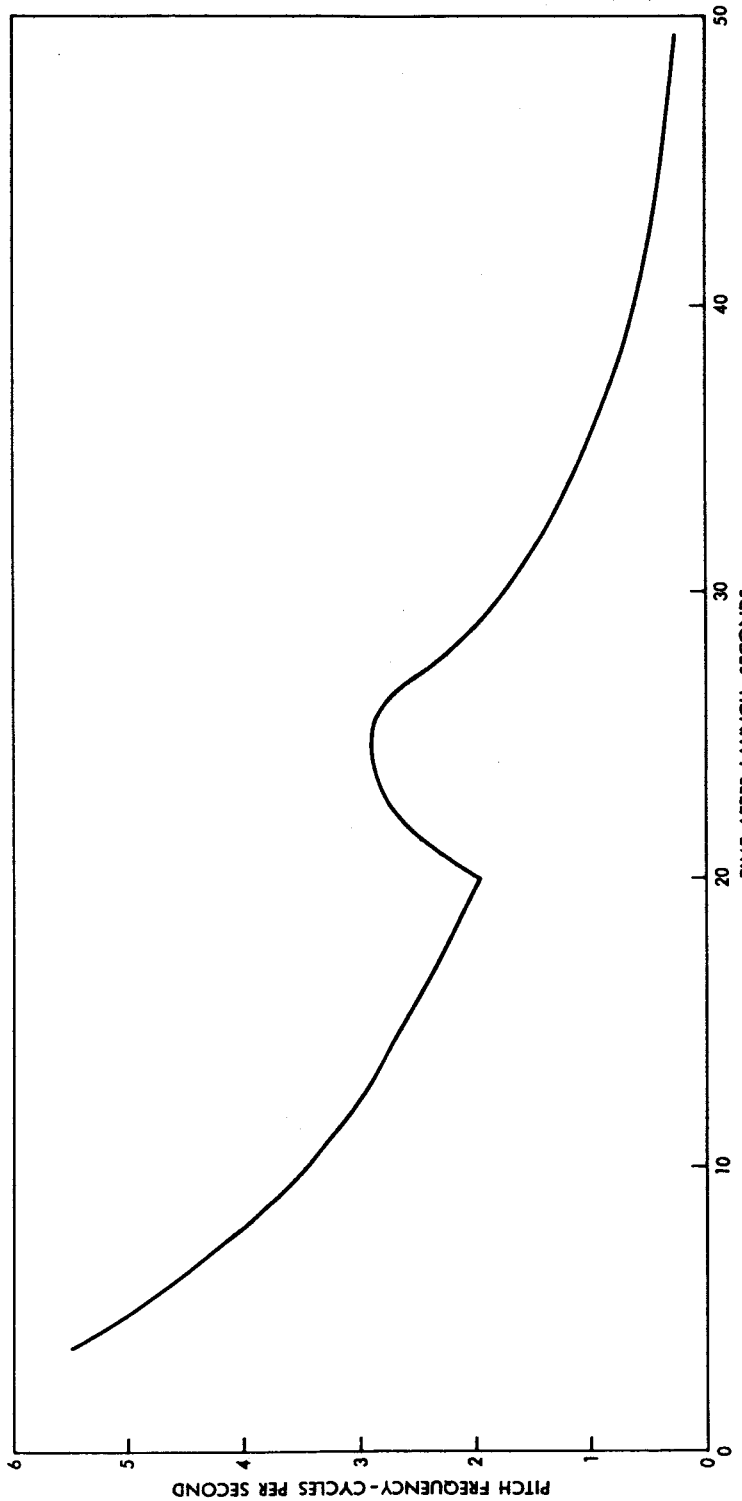

Figure 3 - Theoretical Rigid Body Apache Pitch Frequency

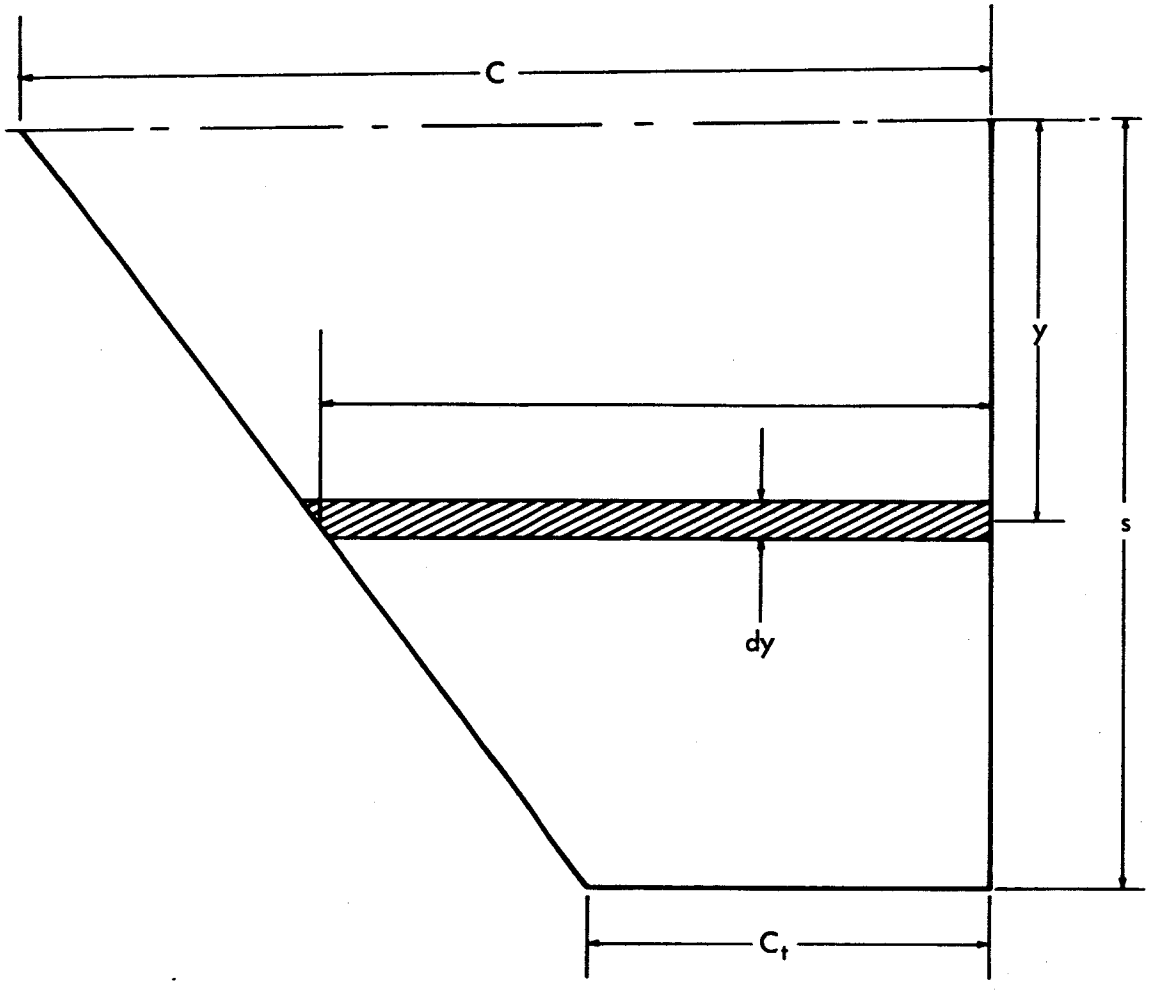

Figure 4- Strip Theory On Fins

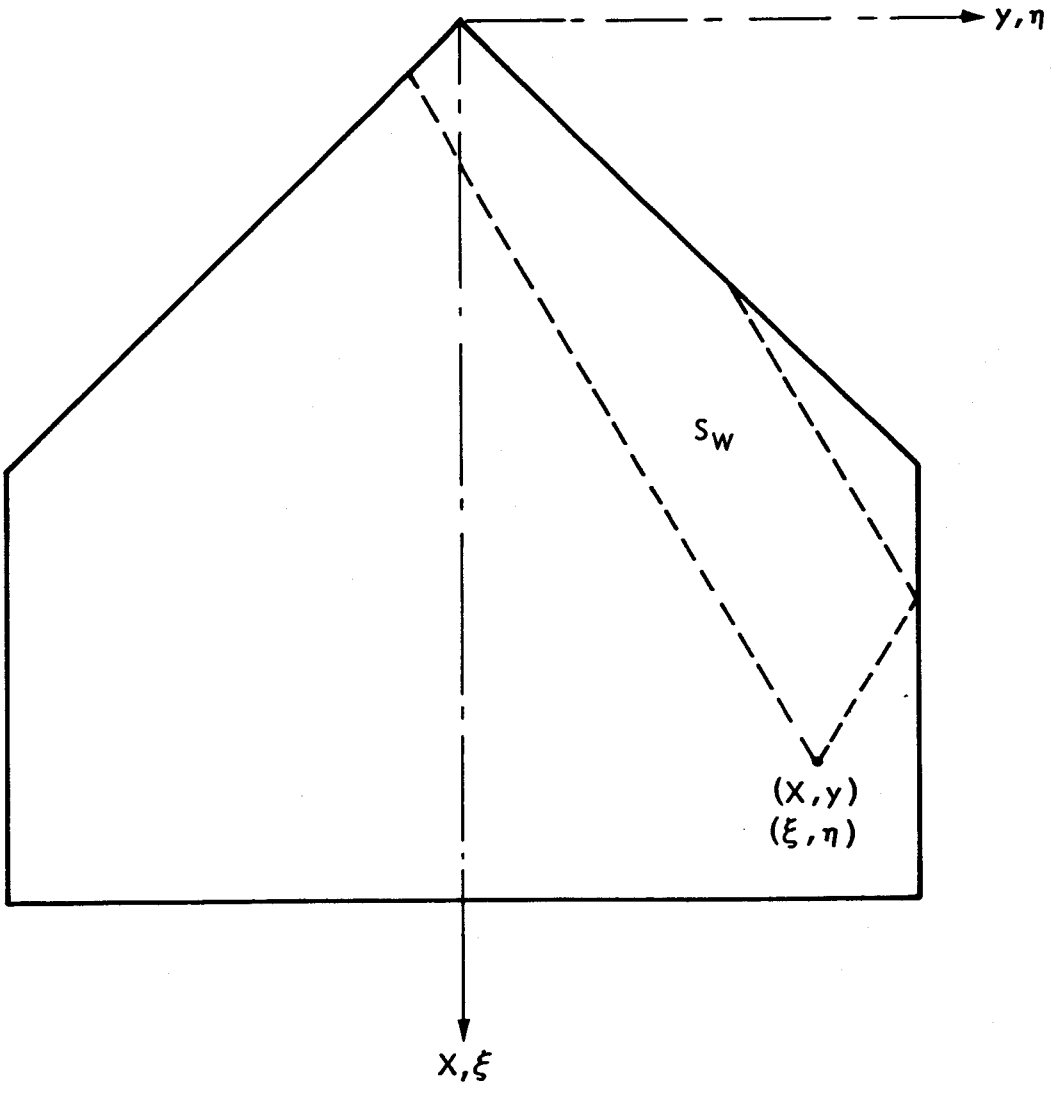

Figure 5 - Coordinate System on Fin

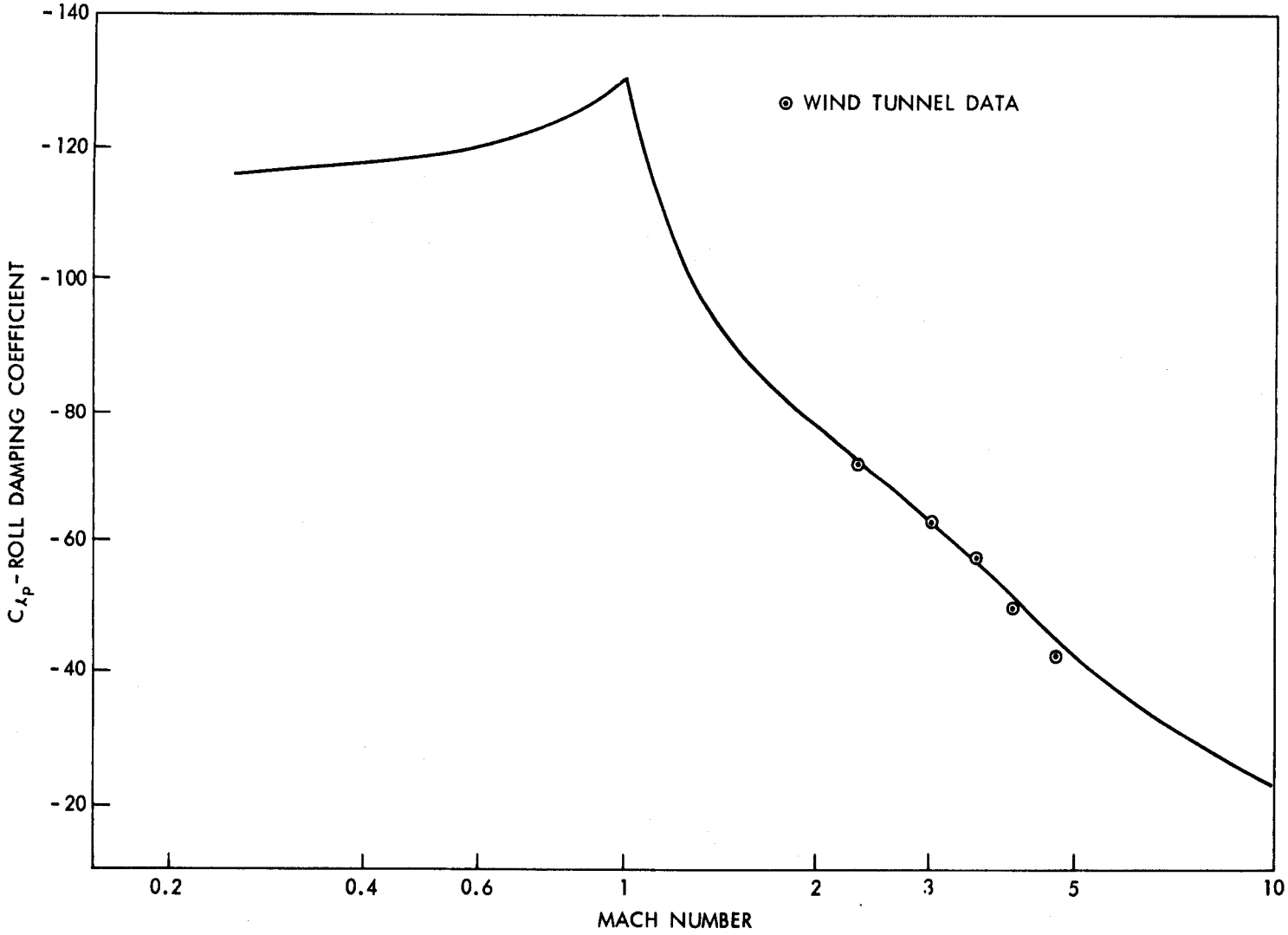

Figure 6- Theoretical Roll Damping Coefficient

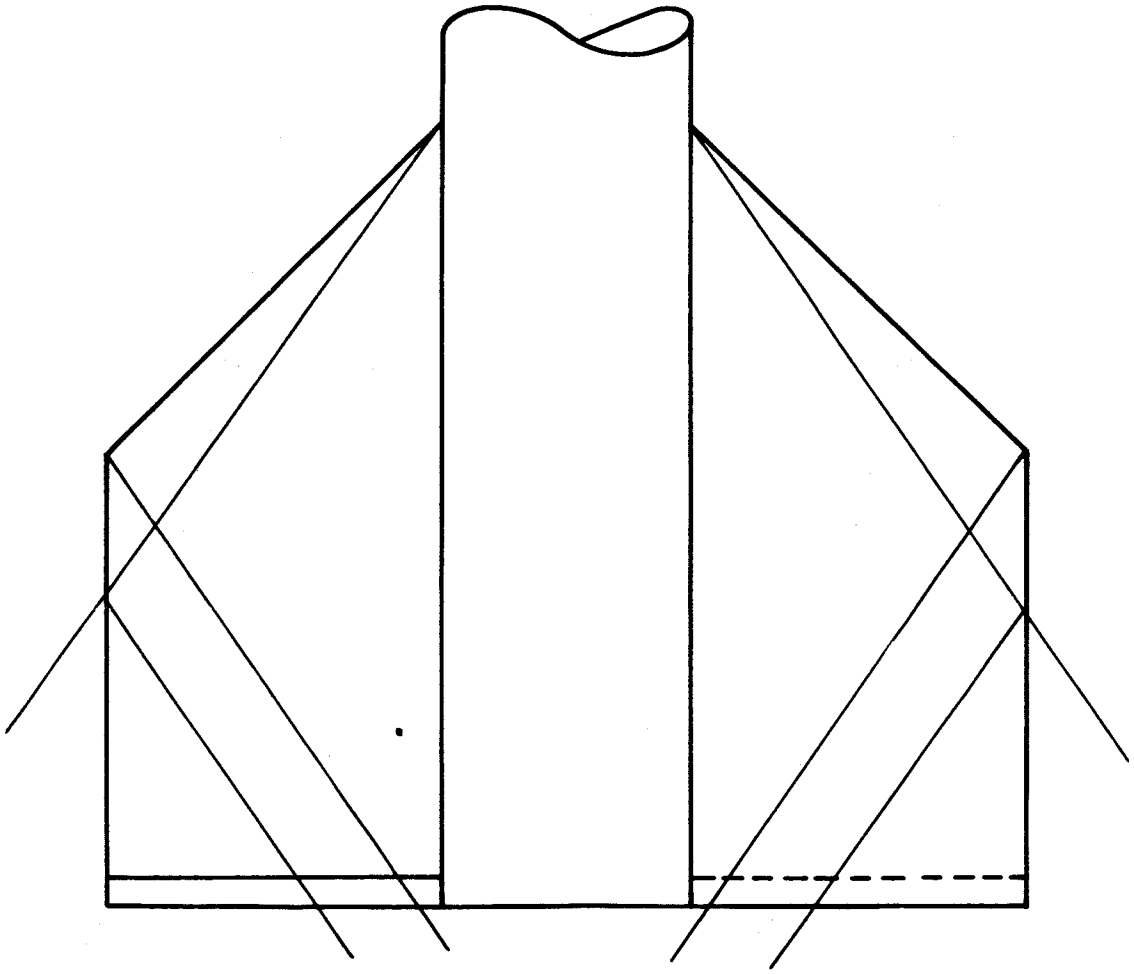

M=1.75

Figure 7a - Mach Lines for Flow Over Fin

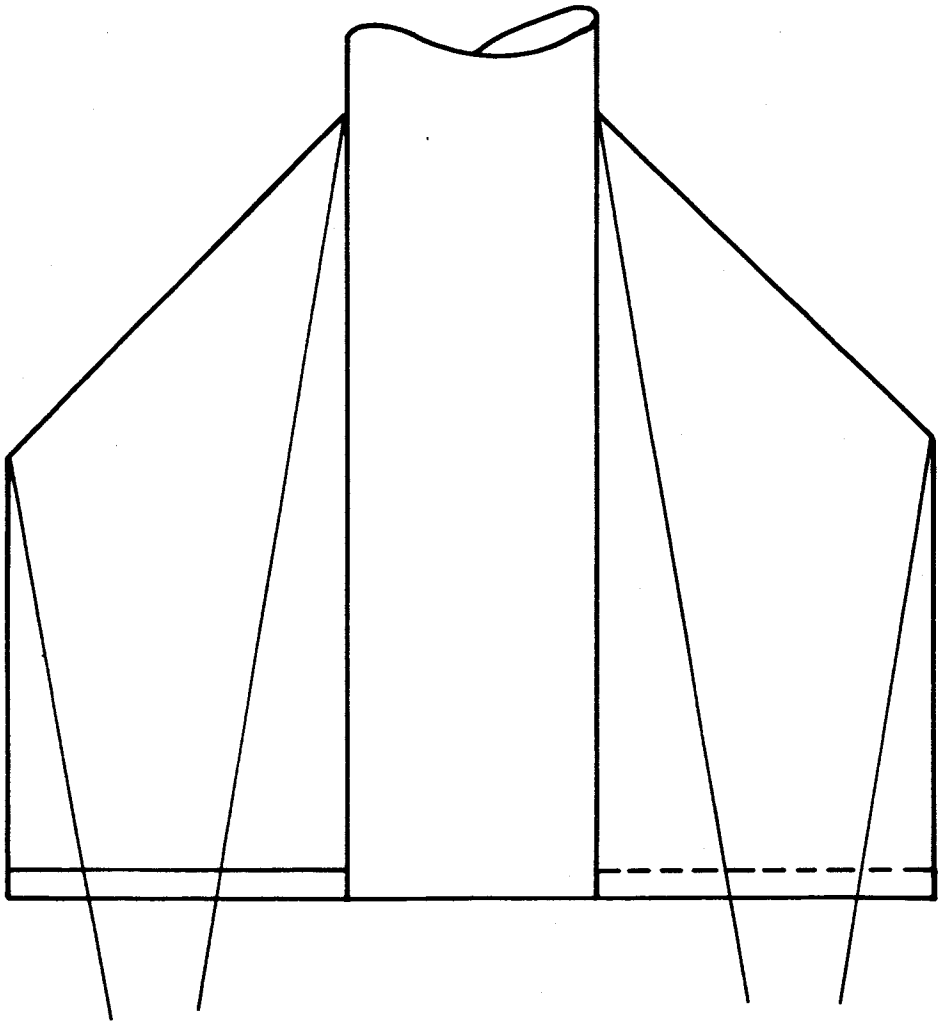

M=6.0

Figure 7b - Mach Lines for Flow Over Fin

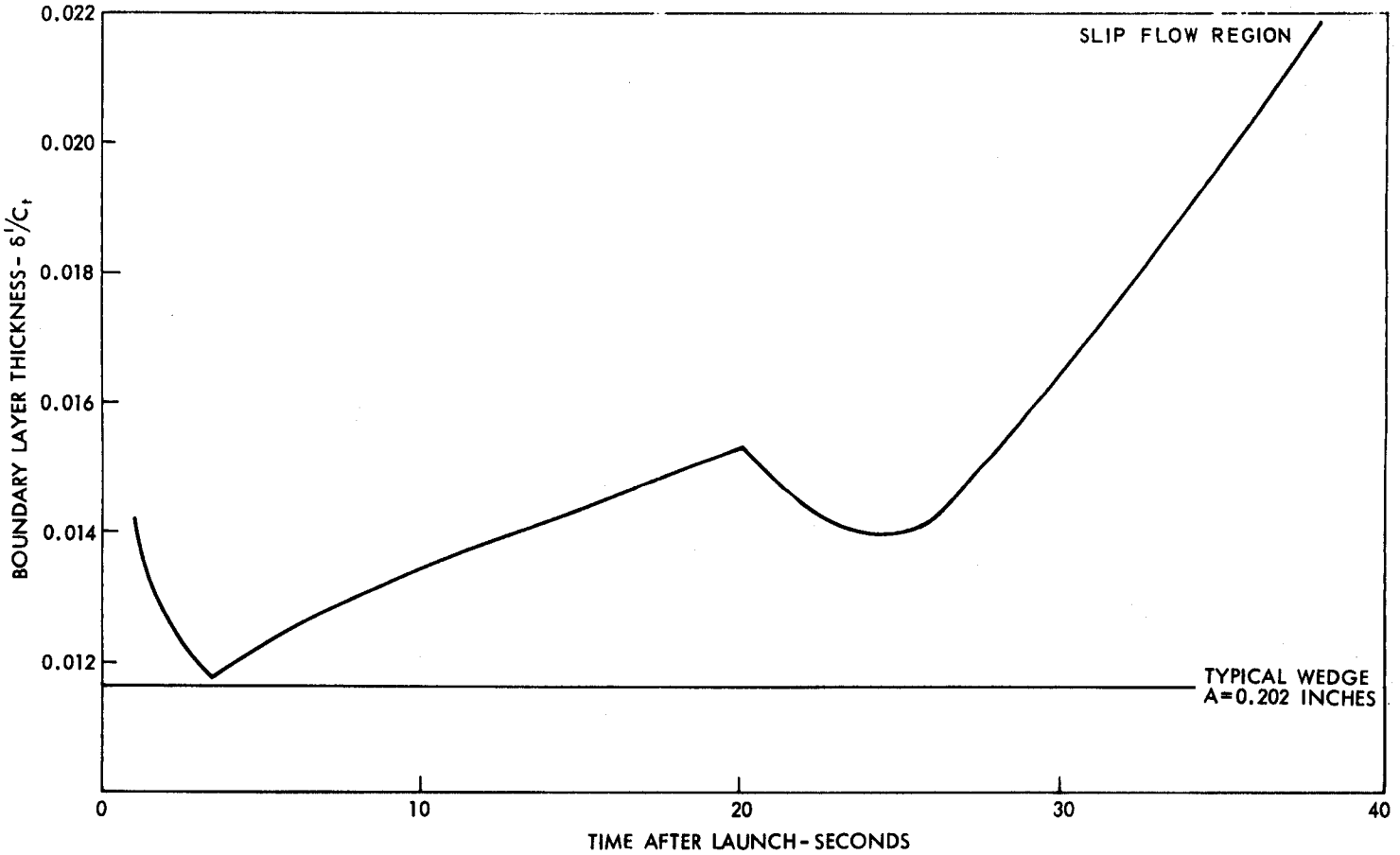

Figure 8 - Boundary Layer Thickness At Trailing Edge Of Fin, Typical Apache Trajectory

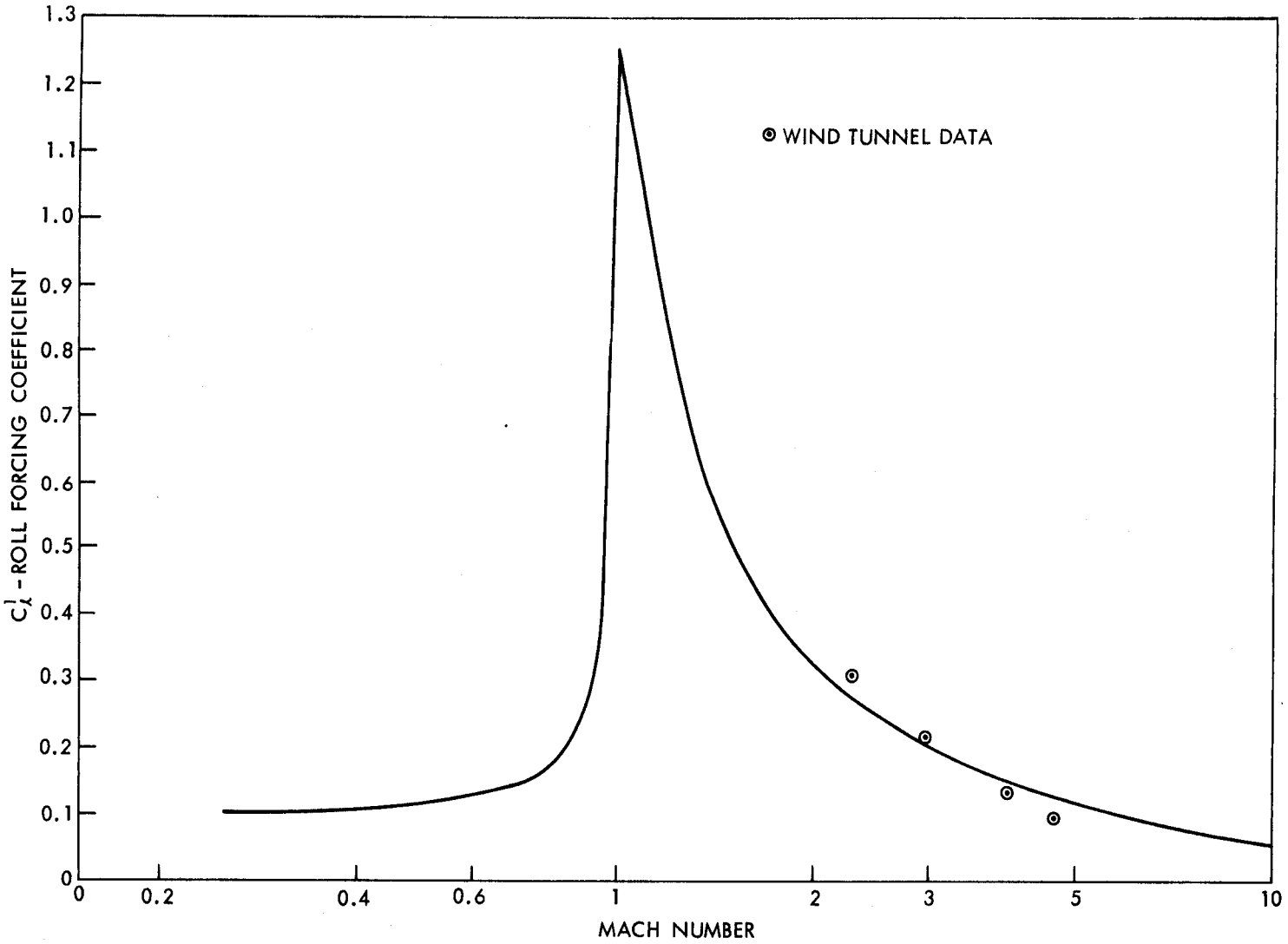

Figure 9 - Theoretical Roll Forcing Coefficient; $\delta = 8°$, $h = 1.5$ inches

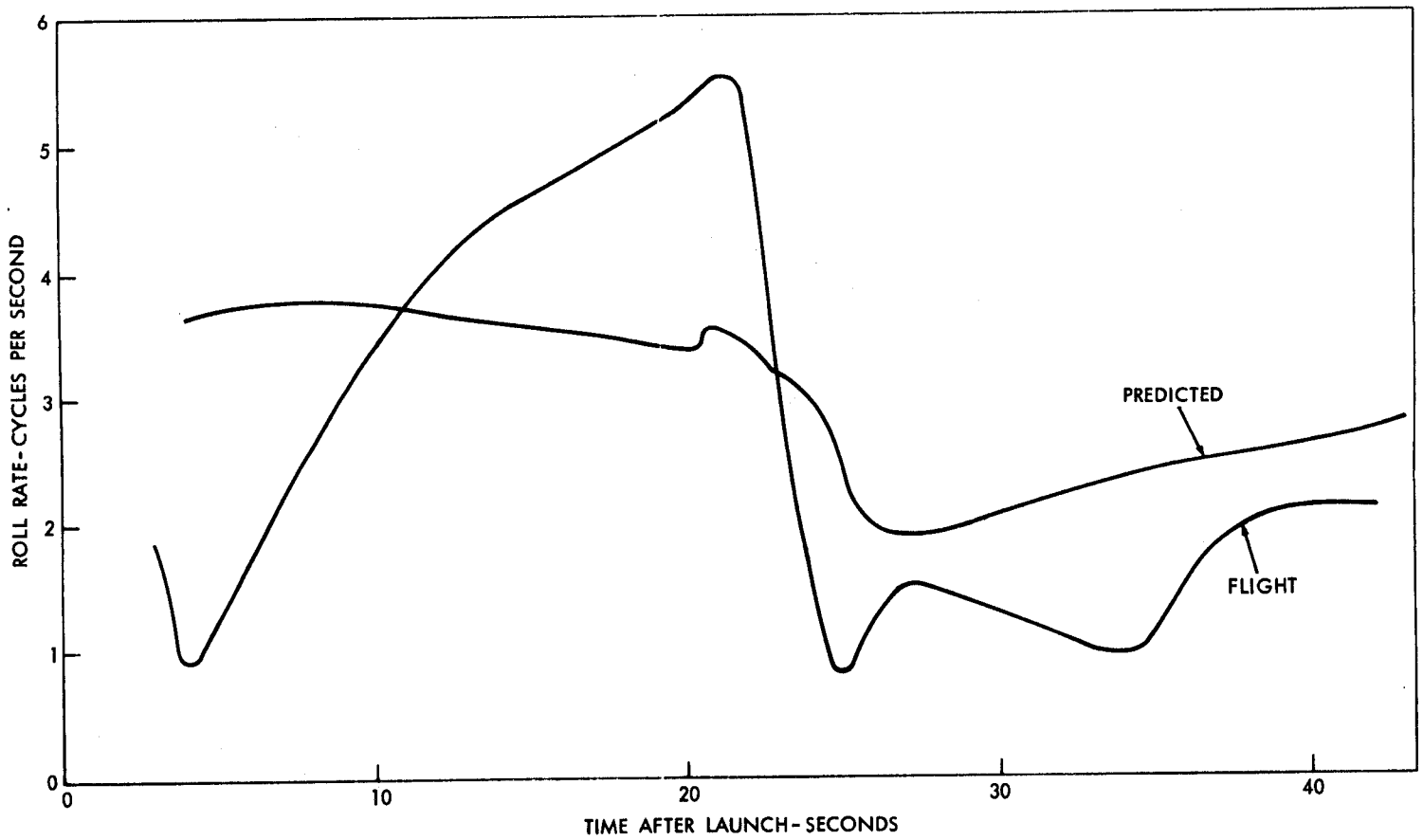

Figure 10- Flight Roll Rate Nike-Apache 14.150 Launched 15 Jan. 1964; $\delta = 10.6°$, $h = 0.75$ inches